A scheme-fitted splitting method for source terms to solve inhomogeneous Maxwell equations in time domain

Bruno Fornet

A scheme-fitted splitting method for source terms to solve inhomogeneous Maxwell equations in time domain

B. Fornet
NUCLETUDES, 3 avenue du Hoggar
- Les Ulis -CS 70117-
91978 Courtabœuf Cedex - France

May 24, 2012

Abstract

In this article, we construct a family of solutions to nonhomogeneous Maxwell equations for which numerical computations exhibit an unphysical behavior for a number of tested schemes (FDTD, FVTD, and several DGTD schemes), the current density source term being discretized like the electrical field. We then propose a new, scheme-fitted method to account for this source term, resulting in the correction of the forementioned numerical results for all tested schemes. Doing so provides a new insight on test cases used in the framework of divergence cleaning techniques. The proposed method is based on Helmholtz Theorem. A general theoretical result, dictated from considerations at a continuous level, is given as a hint to explain the drastic and indiscriminate improvement numerically observed.

Keywords:. *Maxwell equations, Divergence constraints, Charged cavity, Discontinuous Galerkin Methods, Charge conservation*

1 Introduction

We recall adimensionalized Maxwell equations with source terms (ρ, J) in a square metallic box of dimension one ($\Omega = [0,1]^3$):

$$\begin{cases} \partial_t E - \nabla \times H = -J, \ (t,x) \in (0,T) \times \Omega, \\ \partial_t H + \nabla \times E = 0, \ (t,x) \in (0,T) \times \Omega, \\ \nabla . E = \rho, \ (t,x) \in (0,T) \times \Omega, \\ \nabla . H = 0, \ (t,x) \in (0,T) \times \Omega, \\ \partial_t \rho + \nabla . J = 0, (t,x) \in (0,T) \times \Omega, \\ E|_{t=0} = E_0, \ x \in \Omega, \\ H|_{t=0} = H_0, \ x \in \Omega, \\ n \times E|_{\partial\Omega} = 0. \end{cases} \tag{1.1}$$

Numerically, the equations actually solved are:

$$\begin{cases} \partial_t E - \nabla \times H = -J, \ (t,x) \in (0,T) \times \Omega, \\ \partial_t H + \nabla \times E = 0, \ (t,x) \in (0,T) \times \Omega, \\ E|_{t=0} = E_0, \ x \in \Omega, \\ H|_{t=0} = H_0, \ x \in \Omega, \\ n \times E|_{\partial\Omega} = 0. \end{cases} \tag{1.2}$$

This system is written while still assuming the constraint on the data $\partial_t \rho + \nabla . J = 0$ to be satisfied for all $(t,x) \in (0,T) \times \Omega$.

We restrict ourselves voluntarily to the framework of explicit time schemes, which are suited for hyperbolic problems due to the non so restrictive stability condition associated (compared to parabolic ones).

Numerically, whether homogeneous Maxwell equations are solved or whether source terms are present, the quality of the solutions obtained can be quite different, even in the well-known setting of a cubic metallic cavity. Strikingly nonphysical electromagnetic fields can be easily achieved in a well-known 2D transverse electric case from Issautier ([9]) through "classical schemes", well-behaved in the sourceless divergence free case.

So far as the simulation of Maxwell equations is concerned, divergence constraints are not discretized. Moreover, most proofs about the numerical satisfaction of Gauss law are done in a divergence-free case.

As a consequence, nonphysical solutions, such as the ones observed in [9], are often called spurious and linked to divergence problems ([11]). The association of ideas between the errors arising in these cases and divergence errors are so deep rooted that, in [9] and [15], quantization of the numerical error is only done on the divergence of the electromagnetic fields, and not the fields themselves. The observed behaviors, if analyzed this way only,

thus strongly encourage the use of correction methods. That is why, in [15], the authors propose a 3D variant of the Issautier case in order to try out hyperbolic divergence cleaning techniques. In [8], the systematic use of a divergence cleaning method is even recommended as far as nonhomogeneous Maxwell's equations are concerned. Some correction methods used for divergence cleaning are studied in detail in [9] and [7]. They are also analyzed in a Maxwell-Vlasov framework in [12] and [10].

In this article, we show that, for the considered cases, qualitatively analogous to the one of Issautier, divergence pollution is not caused by the chosen schemes but rather by errors in the computation of the electrical field due to the methodology of discretization used for the source terms. Hence the previously considered examples no longer hint towards the systematic use of a divergence cleaning method for the numerical computation of nonhomogeneous Maxwell's equations.

We first construct another, more explicit, family of 3D periodic solutions similar to the ones used when testing the efficiency of divergence cleaning techniques ([9],[15]). They are volumic source terms creating self-sustained fields with modal structure. The fully explicit nature of the constructed solutions will allow a thorough analysis of the behavior of the associated numerical solutions.

Let us explain in a few words:
Going back to Maxwell-Ampère equation:

$$\partial_t E - \nabla \times H = -J,$$

a first logical attempt, often adopted in computational electromagnetism, is to discretize E and J the same way. By exhibiting corresponding numerical simulations, we show that, by doing so, for all tested schemes, which ensure correct (up to the scheme order) solutions for the homogeneous divergence-free case, strongly nonphysical fields can be easily excited. The tested schemes include finite volumes and Yee finite difference schemes. In many cases, the periodic character of the computed solution is not retained as time goes by, in others the periodic character is retained but an abnormal noise can arise.

We then propose a systematic scheme-fitted method to account for source terms, which completely rids the numerical solutions from any unphysical behavior for every tested schemes. The key is, using a Hodge decomposition, to introduce the source term of the equation in a scheme-conforming way, namely in adequation with the discretization made of $\nabla \times H$ rather than with the one made of E. Since this method applies for any numerical scheme,

we choose to test it on both schemes coming from a variational approach and on a finite difference scheme.

In **Section** 2, we show that unphysical fields may numerically arise for a divergence free nonhomogeneous case. We continue by giving in **Section** 3 the usual (but not always correct) scheme-independent way to account for source terms of current, which was used for the simulation exposed in **Section** 2.

Then, in **Section** 4, we present the proposed method based on a Hodge decomposition of the source terms. We show that, under some assumptions, we can, by using a suitable splitting of the equations and change of unknowns, formally go back to a homogeneous system through the use of this method. This could explain why numerical results obtained by our approach seem to retain the quality usually observed when computing the solution to homogeneous Maxwell's equations. The **Section** 4 exposing this matter could be viewed as a sketch of proof. We have deliberately chosen to keep it this way, in order to emphasize the simplicity and the generality of the method, rather than choosing a specific scheme, and attempting to get more formal results. In the same mindset, solution curves are directly given to the reader. Among the tested schemes are the Yee FDTD scheme, finite volume scheme, and first order DGTD schemes with general fluxes. In the appendix, more precisions can be found concerning the encoded schemes.

Section 5 is devoted to the construction of the cases used for the numerical investigation.

All numerical tests consist in showing the time history of the fields at a given point, comparing the exact solution to the computed ones with source terms taken into account by the methods presented respectively in **Section** 3 and in **Section** 4. Since increasing the order of the scheme or using a full upwind flux just decreases the velocity of the unphysical drift (a vertical monotonous drift breaks the field time periodicity), we choose to only show the result of simulations for low order (up to one) and centered schemes. Observing this kind of behavior, one legitimate question would be to know if our method completely corrects the fields, in the sense that nonperiodic fields may arise on larger time scales. Numerical tests, performed during millions of temporal iterations, still show no unphysical behavior. For the DGTD schemes of order one, we try both nodal (Lagrange) and modal (Legendre) basis functions. We refer the reader to [5] for a review on DGTD methods. Our numerical tests are divided into two parts. A $3D$-variant of the case proposed in $2D$ by Issautier ([9]) was numerically explored first in **Section** 6.

In **Section** 7, we then test an associated divergence free case (obtained

from Hodge decompositions). For this purpose, we introduce basis functions Q^1_{div} proposed by Nedelec in [13] (see [2] for their use in a DGTD framework) and P^1_{div} ([3]). Both are built to satisfy special properties with respect to divergence. Note that the P^1_{div} basis functions are locally divergence free basis functions like the ones introduced in [6]. These special basis functions significantly decrease the drift velocity but do not correct it, although using our method to account for source terms does.

We then go back to the case proposed and tested in [4]. In **Section** 8, we demonstrate through an example that the quality of convergence achieved is far from normal, although unperiodic solutions do not arise in this case.

Before concluding, we underline in **Section** 9, that the errors numerically observed on the electrical fields are actually polarized with respect to Hodge decomposition. To sum up, on a discrete level, they pollute $\nabla.E$, whereas they have no consequence on $\nabla \times E$.

2 Possibility of unphysical numerical drift in a divergence free case

A logical question is to know whether unphysical numerical results observed for the family of cases developed in this paper are linked to the presence of a nonzero density of charge ρ. The following case, associated to the parameters $\alpha = 0$ and $\beta = 1$ (see **Section** 5), is such that $\rho = 0$, causes both electromagnetic fields to be divergence free. Except if precised otherwise, a same $10 \times 10 \times 10$ cartesian mesh is used to perform all the numerical cases exposed in this article. Using a discontinuous Galerkin method with Lagrange nodal functions of first order, with centered fluxes and a fourth order Runge Kutta time scheme, the numerical result represented in Figure 1 demonstrates that unphysical behavior may arise even for $\rho = 0$.

3 Direct discretization of the source terms in the approximation space of the electrical field

The source terms of Yee FDTD scheme are usually taken as described in [16] (pages 64–65), that is to say that J is discretized the same way as the field E.

For DGTD schemes with Lagrange basis functions, the degrees of freedom of the source term are obtained by direct evaluation on the corresponding node of the mesh. Referring to **Section** A.1 for the notations employed;

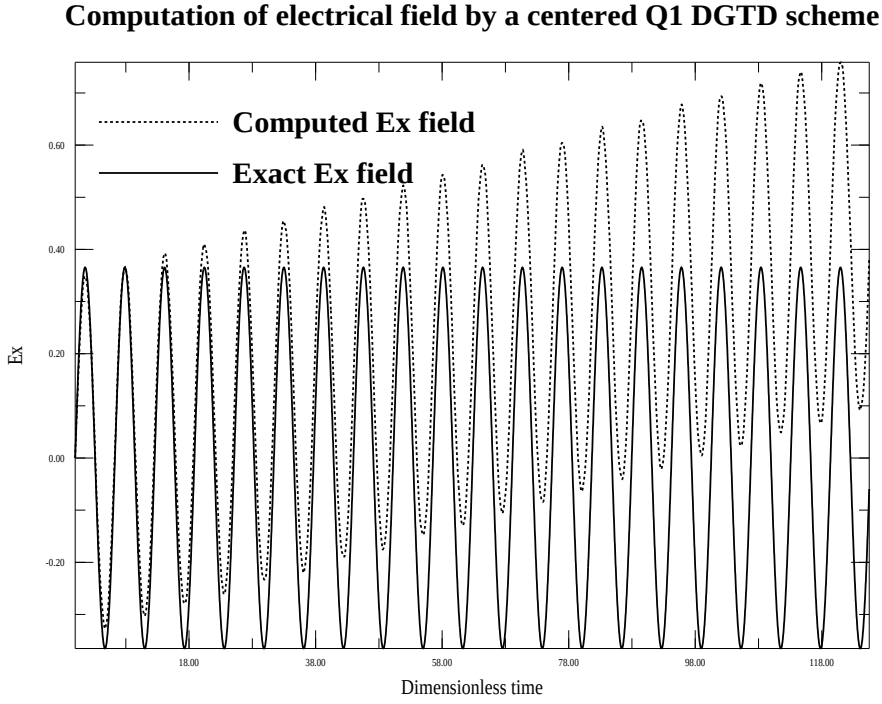

Figure 1: Abnormal non periodic behavior for a RK4/Q1 DGTD scheme for a divergence free exact solution.

in general, for all DGTD schemes, the formula:

$$u_K(t,x,y,z) = \sum_{i=1}^{n_U^K} \mathcal{U}_i^K(t)\psi_{\mathcal{U},i}^K(x,y,z)$$

allows to recover at any given time $\mathcal{U}_i^K$ from u_K by doing:

$$(\mathcal{U}_i^K)_{1\leq i\leq n_U^K} = Mass^{-1}\left(\int_{\Omega_K} \langle u_K, \psi_{\mathcal{U},i}^K\rangle \, d\mu\right)_{1\leq i\leq n_U^K}$$

where $Mass$ denotes the mass matrix given by:

$$Mass = \left(\int_{\Omega_K} \langle \psi_{\mathcal{U},i}^K, \psi_{\mathcal{U},j}^K\rangle \, d\mu\right)_{1\leq i,j\leq n_U^K}.$$

4 Description of the method and guidelines of proof

We can numerically split the resolution of Maxwell equations in time without major drawback (see [1]). It is particularly interesting when considering the Maxwell system decomposed along its transverse and longitunal parts, one gets:

$$\begin{cases} \partial_t E_{grad} = -J_{grad},\ (t,x) \in (0,T)\times\Omega, \\ \nabla.E_{grad} = \rho,\ (t,x) \in (0,T)\times\Omega, \\ E_{grad}|_{t=0} = E_{grad,0},\ t \in (0,T), \\ \partial_t E_{rot} - \nabla\times H_{rot} = -J_{rot},\ (t,x) \in (0,T)\times\Omega, \\ \partial_t H_{rot} + \nabla\times E_{rot} = 0,\ (t,x) \in (0,T)\times\Omega, \\ E_{rot}|_{t=0} = E_{rot,0}, H_{rot}|_{t=0} = H_{rot,0},\ t \in (0,T), \\ n\times E_{rot}|_{\partial\Omega} = 0,\ (t,x) \in (0,T)\times\partial\Omega, \\ H_{grad} = 0,\ (t,x) \in (0,T)\times\Omega. \end{cases} \tag{4.1}$$

Each field $\mathbf{U}$, where $\mathbf{U}$ stands for E, H, or J, has its Hodge decomposition:

$$\mathbf{U} = \mathbf{U}_{grad} + \mathbf{U}_{rot},$$

where $\nabla\times\mathbf{U}_{grad} = 0$, and $\nabla.\mathbf{U}_{rot} = 0$.

Let us stress that, if $(E_{grad}, E_{rot}, H_{grad}, H_{rot}, J_{grad}, J_{rot})$ satisfy the decoupled system (4.1), then $E := E_{grad} + E_{rot}$ and $H := H_{grad} + H_{rot}$ are solution of the Maxwell system with $J := J_{grad} + J_{rot}$ as the current source term.

We want to investigate the link between the treatment of source terms and the choice for the spatial discretization of the operators. To do so, we will only focus here on the spatial features of the current sources rather than on their temporal behaviors. It is an assumption very pertinent with regard to the family of cases we choose to study in this article, and the numerical behavior they exhibit. One sees in the splitted system 4.1, that E_{grad} has no connection with the choice of the *curl* discretization by the space scheme, nor the metallic boundary condition. On the other hand, E_{grad} is the only unknown to be involved in Gauss' law. Our choice is then to rather focus on the reduced problem:

$$\begin{cases} \partial_t E_{rot} - \nabla\times H_{rot} = -J_{rot},\ (t,x) \in (0,T)\times\Omega, \\ \partial_t H_{rot} + \nabla\times E_{rot} = 0,\ (t,x) \in (0,T)\times\Omega, \\ n\times E_{rot}|_{\partial\Omega} = 0,\ (t,x) \in (0,T)\times\partial\Omega, \\ E_{rot}|_{t=0} = E_{rot,0}, H_{rot}|_{t=0} = H_{rot,0},\ t \in (0,T). \end{cases} \tag{4.2}$$

We conclude then by the following formal but far reaching result:

Proposition 4.1. *Let us assume that $\partial_t J_{rot} = 0$, then solving the system 4.2 is formally equivalent to solving the homogeneous system.*

Proof. The Hodge decomposition of J writes:

$$J = J_{rot} + J_{grad} = \nabla \times J_{\nabla\times} + \nabla J_{\nabla}.$$

It suffices then to remark that $(E_{rot}, H_{rot} - J_{\nabla\times})$ is solution of the associated sourceless problem with metallic boundary conditions. □

Rather than trying to prove the Theorem suggested by this proposition through a proper numerical analysis for a given scheme, we prefer to test numerically for different schemes the logical link we traced between the original Maxwell system and this Proposition.

Going back to the initial set of equations, for an explicit in time resolution scheme, Proposition 4.1 infers the following scheme-fitted method to treat a source term:

$$\begin{cases} (\partial_t E)_{t-scheme} - (\nabla \times H)_{s-scheme} = -(\nabla \times J_{\nabla\times})_{s-scheme} - J_{grad}, \ (t,x) \in (0,T) \times \Omega, \\ (\partial_t H)_{t-scheme} + (\nabla \times E)_{s-scheme} = 0, \ (t,x) \in (0,T) \times \Omega, \end{cases} \tag{4.3}$$

where $t - scheme$ denotes the chosen time scheme whereas $s - scheme$ is used to refer to the chosen space scheme. We thus mean that we discretize $\nabla \times J_{\nabla\times}$ the same way as we do for $\nabla \times H$ by choosing a given scheme. For the exposed numerical results, J_{grad} was taken into account as described in **Section** 3.

5 Construction of a family of explicit solutions for Maxwell equations with nontrivial source terms

For the sake of simplicity let us assume in what follows that $\varepsilon_0 = \mu_0 = c = 1$. In [9], Issautier gives the following example of explicitly constructed electromagnetic fields $(TE)_z$ in the presence of charges. The corresponding perfect electric cavity ranges from 0 to 1 in each space dimension.

$$E = sin(t) \begin{pmatrix} xsin(\pi y) \\ ysin(\pi x) \\ 0 \end{pmatrix}$$

$$H = (cos(t) - 1) \begin{pmatrix} 0 \\ 0 \\ \pi y cos(\pi x) - \pi x cos(\pi y) \end{pmatrix}.$$

The associated charge and current densities are:

$$\rho = sin(t)(sin(\pi x) + sin(\pi y))$$

$$J_x = (cos(t) - 1)\left(\pi cos(\pi x) + \pi^2 x sin(\pi y)\right) - x cos(t) sin(\pi y)$$
$$J_y = (cos(t) - 1)\left(\pi cos(\pi y) + \pi^2 y sin(\pi x)\right) - y cos(t) sin(\pi x)$$

In [15], the authors introduce an extension of the Issautier case to 3D. They only give the expression of the density of charge and current (not those of the associated electromagnetic fields), that is to say:

$$\rho = sin(t)(sin(\pi z) + sin(\pi x) + sin(\pi y))$$
$$J_x = (cos(t) - 1)\left[\pi cos(\pi x) + \pi^2 x sin(\pi z)\right] - cos(t) x sin(\pi z)$$
$$J_y = (cos(t) - 1)\left[\pi cos(\pi y) + \pi^2 y sin(\pi x)\right] - cos(t) y sin(\pi x)$$
$$J_z = (cos(t) - 1)\left[\pi cos(\pi z) + \pi^2 z sin(\pi y)\right] - cos(t) z sin(\pi y)$$

The corresponding fields are not trivial to obtain since the natural modal candidates:

$$E = sin(t) \begin{pmatrix} x sin(\pi z) \\ y sin(\pi x) \\ z sin(\pi y) \end{pmatrix}$$
$$H = -(cos(t) - 1) \begin{pmatrix} \pi z cos(\pi y) \\ \pi x cos(\pi z) \\ \pi y cos(\pi x) \end{pmatrix}$$

do not verify the perfect metallic boundary conditions.

We thus prefer to consider the following variant, constructed from an explicit 3D solution proposed in [4]. Note that the reduction to 2D of this variant exhibits the same unphysical behavior as the case of Issautier.

In what follows, we construct a family of solutions to the nonhomogeneous Maxwell system parametrized by the real numbers α and β. The dependence of the variables towards α and β will be explicited as a superscript for the concerned variable. First, we take

$$J^{\alpha,\beta} = J^{\alpha}_{grad} + J^{\beta}_{rot} = \nabla J^{\alpha}_{\nabla} + \nabla \times J^{\beta}_{\nabla\times}$$

where

$$J^{\alpha}_{\nabla} = \frac{\alpha cos(t)}{2\pi^2}\left(sin(\pi x)sin(\pi y) + sin(\pi y)sin(\pi z) + sin(\pi x)sin(\pi z)\right)$$

and

$$J^{\beta}_{\nabla\times} = \frac{2\pi^2(cos(t) - \beta) - cos(t)}{2\pi} \begin{pmatrix} sin(\pi x)\left(z cos(\pi y) - y cos(\pi z)\right) \\ sin(\pi y)\left(x cos(\pi z) - z cos(\pi x)\right) \\ sin(\pi z)\left(y cos(\pi x) - x cos(\pi y)\right) \end{pmatrix}$$

The associated electric field can also be decomposed into its Hodge decomposition:

$$E^{\alpha} = E^{\alpha}_{grad} + E_{rot} = \nabla E^{\alpha}_{\nabla} + \nabla \times E_{\nabla\times},$$

where $E^{\alpha}_{\nabla} = -\frac{\alpha sin(t)}{2\pi^2}\left(sin(\pi x)sin(\pi y) + sin(\pi y)sin(\pi z) + sin(\pi x)sin(\pi z)\right)$.
The associated magnetic field is:

$$H^{\beta} = \pi(cos(t) - \beta)\begin{pmatrix} sin(\pi x)\left(zcos(\pi y) - ycos(\pi z)\right) \\ sin(\pi y)\left(xcos(\pi z) - zcos(\pi x)\right) \\ sin(\pi z)\left(ycos(\pi x) - xcos(\pi y)\right) \end{pmatrix}.$$

For $\beta = 0$ and $\alpha = 1$, we recover the fields $(E_{Canouet}, H_{Canouet})$ described and tested in [4]. E_{rot} can then be obtained through

$$E_{rot} = E_{Canouet} - \nabla E^1_{grad},$$

where

$$E_{Canouet} = sin(t)\begin{pmatrix} xsin(\pi y)sin(\pi z) \\ ysin(\pi z)sin(\pi x) \\ zsin(\pi x)sin(\pi y) \end{pmatrix}.$$

Note that the associated charge density is:

$$\rho_{Canouet} = sin(t)\left[sin(\pi y)sin(\pi z) + sin(\pi z)sin(\pi x) + sin(\pi x)sin(\pi y)\right].$$

For $\alpha = 1$ and $\beta = 1$ we recover another extension of the Issautier case, the corresponding J, which is written:

$$J^{1,1} = \begin{pmatrix} \pi(cos(t) - 1)cos(\pi x)(sin(\pi z) + sin(\pi y)) + (2\pi^2(cos(t) - 1) - cos(t))xsin(\pi y)sin(\pi z) \\ \pi(cos(t) - 1)cos(\pi y)(sin(\pi x) + sin(\pi z)) + (2\pi^2(cos(t) - 1) - cos(t))ysin(\pi z)sin(\pi x) \\ \pi(cos(t) - 1)cos(\pi z)(sin(\pi y) + sin(\pi x)) + (2\pi^2(cos(t) - 1) - cos(t))zsin(\pi x)sin(\pi y) \end{pmatrix}.$$

6 Numerical results for the case $\alpha = 1$, $\beta = 1$

As discussed before, these parameters correspond to an extension of the Issautier case to 3D.

6.1 Finite volume and first order DGTD schemes

We first begin by showing the behavior of the finite volume scheme and two kinds of classical first order DGTD schemes. Figure 2 shows the fields obtained through the usual method exposed Section 3 while Figure 3 represents those obtained through our method (see Section 4). In Figure 2, the zoom we made in order to show the drift of the fields for the first order methods has truncated some of the information for the finite volume curve as the drift is comparatively too strong. We see that the fields obtained with the splitting of the source term based on a Hodge decomposition do correct the unphysical behavior of the fields (Figure 3). Let us keep in mind that all simulations were voluntarily made on a not so fine mesh, as refining the mesh temporarily hides the problems at hand.

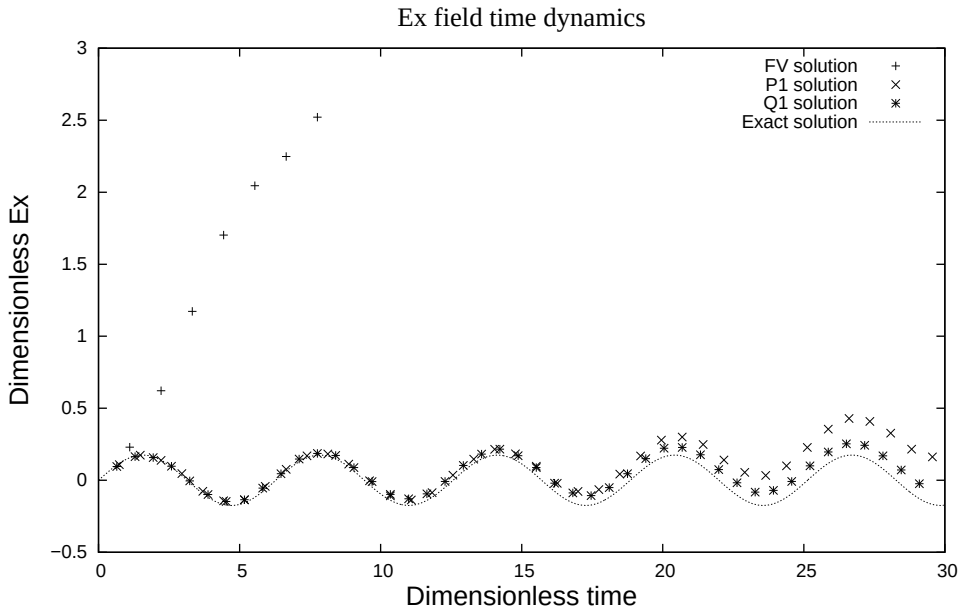

Figure 2: Quick drift on the fields for a 3D extension of the Issautier case

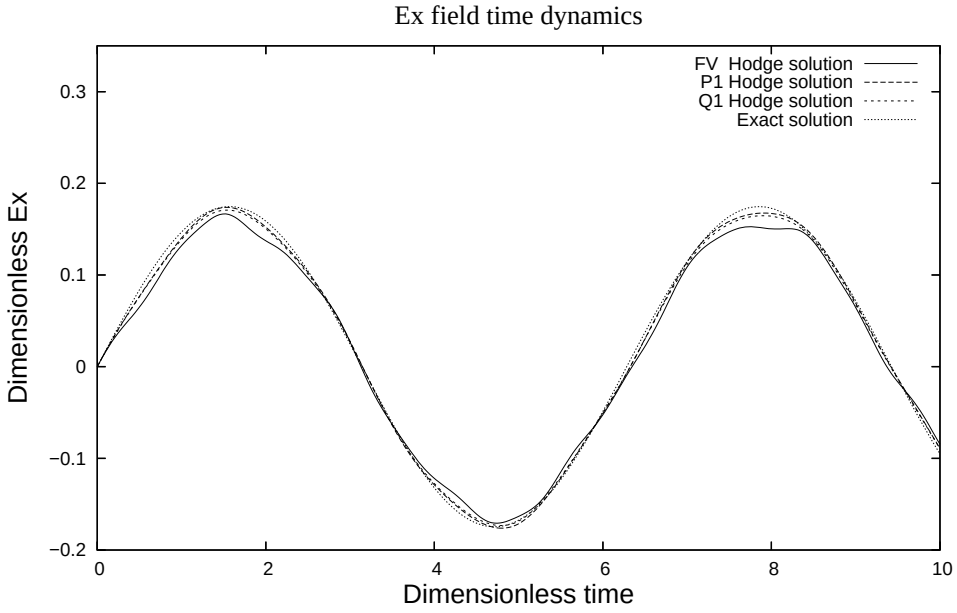

Figure 3: Systematic correction of the fields for a 3D extension of the Issautier case

6.2 Yee finite difference scheme

For the Yee scheme, we compare results given by the source terms treated as suggested in [16] to the ones treated by our method. Once again, we see that the electromagnetic fields are "corrected" in the latter case. This simulation was made independently using another solver, and the observation point was changed, which explains that, this time, the observed field is E_z. A $20 \times 20 \times 20$ mesh was used for this simulation. This case also underlines that the drift occurrence is only linked to the space scheme, since Yee FDTD scheme uses a Leapfrog time scheme.

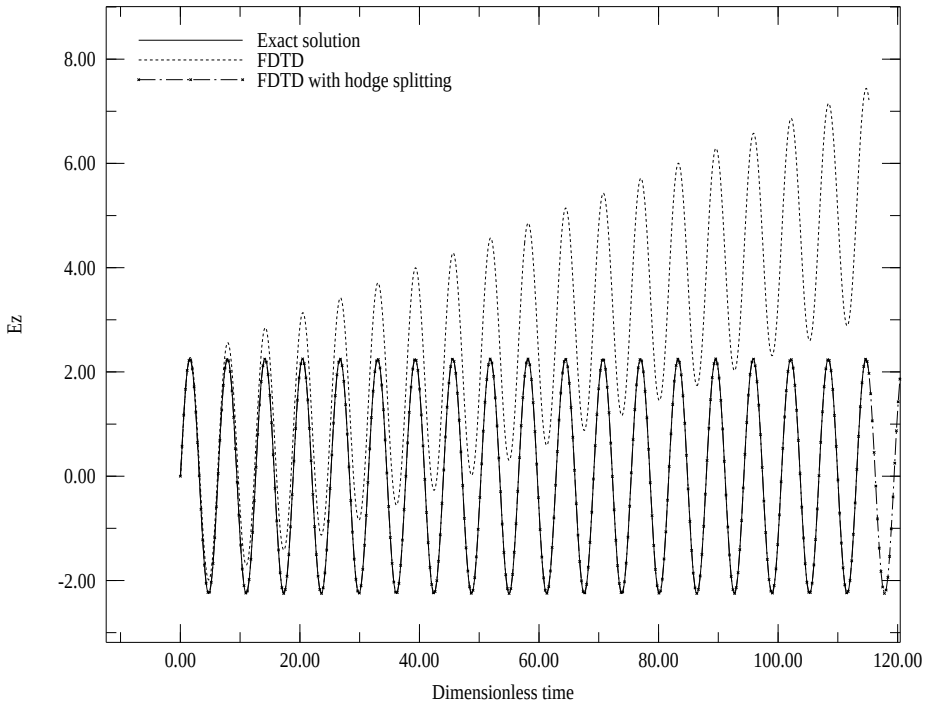

Figure 4: Results obtained for FDTD for both treatments of the source term

7 Results obtained for $\rho = 0$

This case is achieved through the setting $\alpha = 0$ and $\beta = 1$.

7.1 Test with FVTD and usual first order DGTD schemes

As shown in Figure 1, unphysical electromagnetics fields are quickly observed in this setting. As observed before, among $FVTD$, P^1 and Q^1, the Q^1 scheme is the most accurate one.

7.2 Test with first order DGTD schemes wih special divergence properties

Special basis functions (P^1_{div} and Q^1_{div}) have been proposed for the properties they hold. They are bound to present a specially good behavior with regard to the divergence free case. The associated results (with the two ways to account for source terms) are given in Figure 5.

Thanks to these special fonctions, we have to observe the solutions during a longer time frame before the fields drift away significantly (in Figure 5, it is the reason why time begins at 250). However, we show here that the drift is bound to happen. Such a phenomenon can also be observed for a given scheme, when taking a finer mesh or basis functions of higher order, and using full upwind fluxes.

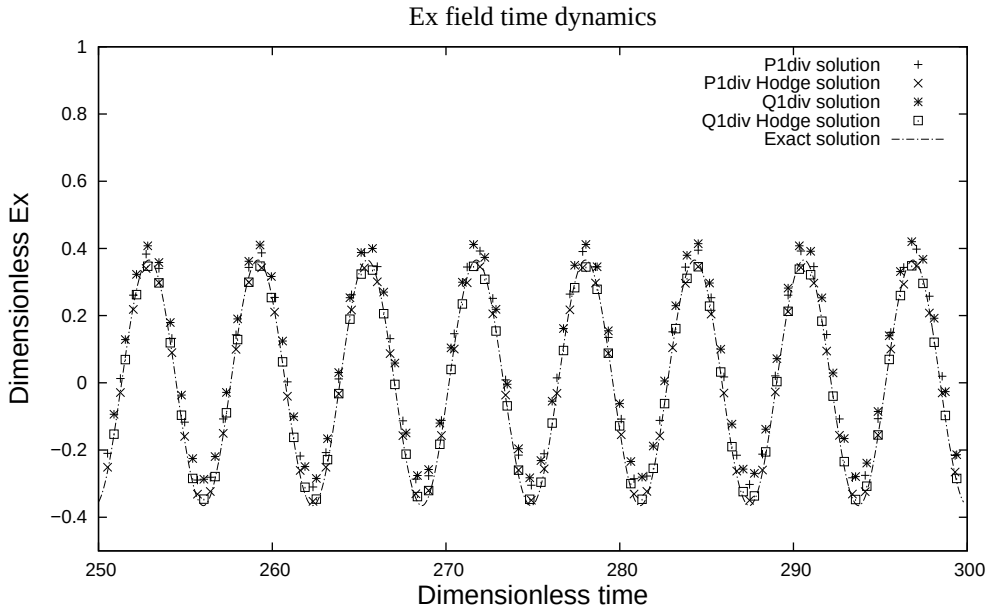

Figure 5: Results obtained for special divergence DGTD schemes

8 Results obtained for the non-deviating case of [4]

This case is achieved through the setting $\alpha = 1$ and $\beta = 0$.

We recall that this case is the one obtained for the setting Using a fine enough mesh and a higher degree of approximation, a small noise remains on the electrical fields while the magnetic ones are correct. Moreover, no drift is observed in this case. Since qualitatively similar results are obtained for finite volumes and other DGTD schemes, we exhibit a most illustrative result for finite volumes. This extreme example is used to show that the observed noise on the electrical fields is still not acceptable.

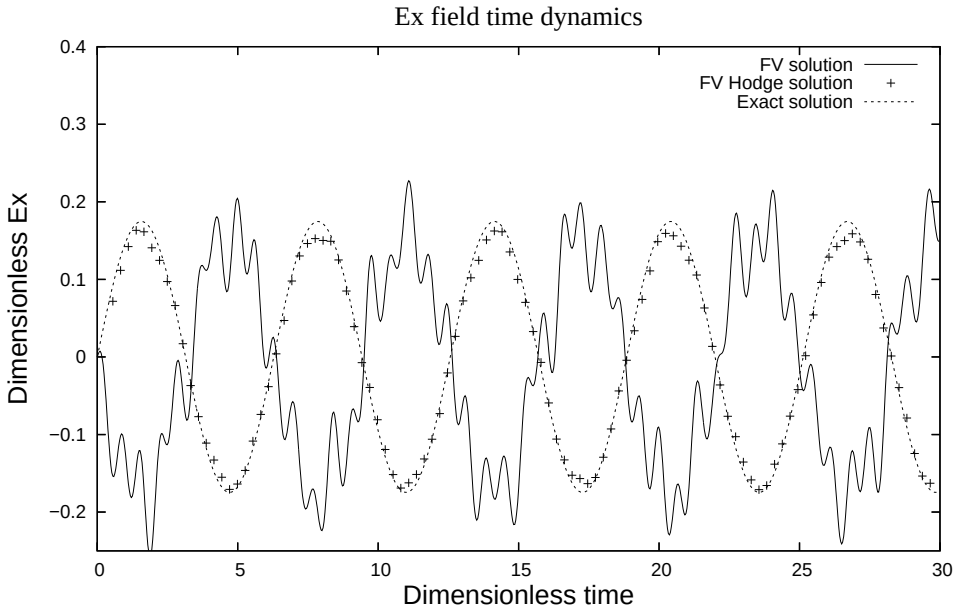

Figure 6: Correction of an abnormal result observed in the case of [4]

9 Polarization of the errors committed when solving inhomogeneous Maxwell's equations

We first begin by a remark made after a careful analysis of the numerical results that we have obtained. Even when the electrical field was exhibiting an unphysical behavior as shown in Figure 1, the magnetic field always remained computed correctly (up to scheme order). This clearly shows that the error committed on the discretized electrical field E remains in the kernel of

$$(\nabla \times .)_{s-scheme}\,.$$

Assuming that the considered scheme enforces the orthogonality property:

$$(\nabla \times [\nabla f])_{s-scheme} = 0,$$

for any sufficiently smooth scalar real function f. Analyzing things with respect to Hodge decomposition, it seems that the committed error is rather connected to 4.2. In addition, this error can be written as $-\nabla\Phi$. As a

result, we could see a link with divergence correction techniques based on an augmented formulation of the form:

$$\varepsilon_0 \partial_t E - \nabla \times H = -J - \nabla \Phi,$$

where Φ is an additional unknown satisfying a suitable equation depending on the choice of the correction method. Note that this comparison is purely formal as the spectral properties of the operator of an augmented system differ from those of the classical Maxwell system. However, we remark that an unphysical error polarized on the rotational part of Hodge decomposition would be unrecoverable.

10 Conclusion

In this paper, we have proposed a general approach based on a splitting of the current source term along a Hodge decomposition. We have successfully tested the proposed process on cases exhibiting nonphysical numerical behaviors. For these cases, errors unaccounted for by the theoretical bounds on the associated homogeneous problem have been observed with several schemes, even for those specifically devised to enforce good divergence properties. These behaviors appear as the consequence of the not careful enough handling of source terms. We have shown as a result that the problem was neither lying with the schemes themselves nor with a "divergence pollution" of the fields. One of the prospective interest of this method is that it suggests that, for some cases at least, the use of costly divergence cleaning techniques can be avoided. One powerful feature is that this method can be tested with any Maxwell solver. Finally, we have shown that the convergence properties of a scheme do not systematically transfer from the homogeneous equations to the nonhomogeneous ones, if the source terms are "just" discretized in the approximation space of the corresponding fields. As a consequence, more intricate methods must be introduced. In this article, a general method is presented to this end. Even if systematically obtaining a Hodge decomposition of the source terms can be costly, the proposed method is interesting for the new insight it provides on the cases studied in this article.

Acknowledgements

The author thanks Matthieu Bonilla and Benjamin Goursaud for fruitful discussions and their contribution to the FDTD aspect of this publication.

References

[1] M.A. Botchev, I. Faragó, R. Horváth, *Application of the operator splitting to the Maxwell equations with the source term*, Memorandum 1818, Department of Applied Mathematics, University of Twente, Enschede, 2007.

[2] A. Bouquet, *Fictitious domain method with a time domain discontinuous Galerkin formulation. Application to antenna modelisation*, PhD Thesis INRIA Sophia Antipolis, 2007.

[3] N. Canouet, L. Fezoui, S. Piperno, *Discontinuous Galerkin Time-Domain solution of Maxwell's equations on locally-refined nonconforming Cartesian grids*, COMPEL, vol. 24, No. 4, 1381–1401, 2005.

[4] N. Canouet, *A discontinuous Galerkin method for solving Maxwell's equation on nonconforming locally refined mesh,* PhD Thesis, Ecole des Ponts ParisTech (2003).

[5] B. Cockburn, G. E. Karniadakis, C.-W. Shu, *The development of discontinuous Galerkin methods* in **Discontinuous Galerkin Methods Theory, Computation and Applications**, Lecture Notes in Computational Science and Engineering, Vol. 11, Springer-Verlag, 3–50, 2000.

[6] B. Cockburn, F. Li, C.-W. Shu, *Locally divergence-free discontinuous Galerkin methods for the Maxwell equations,* J. Comput. Phys. **194**, 588–610, 2004.

[7] B. Fornet, V. Mouysset, A. Rodríguez-Arós, *Mathematical study of a hyperbolic regularization to ensure Gauss' law conservation in Maxwell-Vlasov applications*, Mathematical Models and Methods in Applied Sciences Vol. 22, No. 4 1150020 (28 pages), 2012

[8] E. Gjonaj, T. Weiland, *A divergence cleaning method for the high order DG-FEM in the time domain,* ICEAA 2010 international conference, 581–584, 2010.

[9] D. Issautier, S. Depeyre, *Application aux schémas volumes finis d'une méthode de pénalisation des contraintes pour le système de Maxwell*, rapport de recherche number 95-39, CERMICS, 1995.

[10] G.B Jacobs, J.S. Hesthaven, *Implicit-Explicit Time Integration of a High-Order Particle-in-Cell Method with Hyperbolic Divergence Cleaning*, Comp. Phys. Comm. , 80 (10), 2009.

[11] C.-D. Munz, R. Schneider, E. Sonnendrücker, U. Voß, *Maxwell's equations when the charge conservation is not satisfied*, *C. R. Acad. Sci. paris Sér. I Math.* **328** 431–436, 1999.

[12] C.-D. Munz, P. Omnes, R. Schneider, E. Sonnendrücker, U. Voß, *Divergence correction techniques for Maxwell solvers based on a hyperbolic model*, *J. Comput. Phys.* **161** 484–511, 2000.

[13] J.C. Nédélec, *Mixed finite elements in R3. Numerische Mathematik*, 35(3):315–341, 1980.

[14] J. Rauch, *Symmetric positive systems with boundary characteristic of constant multiplicity*, Transactions of the American Mathematical Society, 291 :167–187, 1985.

[15] A. Stock, J. Neudorfer, R. Schneider, Ch. Altmann, C.-D. Munz, *Investigation of the Purely Hyperbolic Maxwell System for Divergence Cleaning in Discontinuous Galerkin based Particle-In-Cell Methods*, in proceedings of: Coupled Problems 2011 Conference, Kos Island, Greece, June 2011.

[16] A. Taflove, S.C. Hagness, *Computational Electrodynamics: The Finite-Difference Time-Domain Method*, 3rd ed. Artech House Publishers, 2005.

A The numerical schemes used for illustration

A.1 General presentation

For Yee FDTD scheme we refer to [16] and for DGTD schemes we refer to [5]. Maxwell system is a Friedrich's one (see [14]) and writes

$$\partial_t \mathcal{U} + A(\partial)\mathcal{U} = \mathcal{S}, (t,x) \in (0,T) \times \Omega,$$

with assorted suitable (in the sense of [14]) boundary conditions of the form:

$$M\mathcal{U}|_{\partial\Omega} = g,$$

where $A(\partial)$ is a first order symmetric hyperbolic operator. We assume the usual smoothness conditions regarding Ω as well as the datas. We consider a partition of Ω as follows:

$$\Omega = \bigsqcup_{K=1}^{nb_{el}} \Omega_K.$$

The restriction of the unkown $\mathcal{U}$ to the element Ω_K is approximated by:

$$\mathcal{U}|_{\Omega_K}(t,x,y,z) \approx u_K(t,x,y,z) = \sum_{i=1}^{n_U^K} \mathcal{U}_i^K(t)\psi_{\mathcal{U},i}^K(x,y,z).$$

The DGTD solver we use comes from the following variational form in the usual way:

$$(\partial_t\langle\langle u_K, v_K\rangle\rangle)_{RK4} - \langle\langle u_K, A(\partial)v_K\rangle\rangle + \sum_{L\in\nu(K)\setminus bound}\langle\frac{A^\gamma_{out}(n_{KL})}{2}u_L, v_K\rangle$$
$$+\sum_{L\in\nu(K)\setminus bound}\langle\frac{A^\gamma_{in}(n_{KL})}{2}u_K, v_K\rangle + \sum_{L\in bound}\langle(A(n_{KL})-M)u_K + g, v_K\rangle = 0$$

where $A^\gamma_{in} = (1+\gamma)A^+ + (1-\gamma)A^-$ and $A^\gamma_{out} = (1-\gamma)A^+ + (1+\gamma)A^-$. The notation $(.)_{RK4}$ stands for the strong stability preserving Runge-Kutta 4 time scheme we use. This approach allows normal discontinuities of the solution accross the interfaces. While K refers to the current mesh element, L refers to one of its boundaries, the associated normalized outward (with respect to element K) normal is n_{KL}. The notation $\nu(K)$ stands for all the boundaries related to K, there are two kinds of boundaries: the ones associated with boundary conditions and the others. The associated subsets are respectively *bound* and $\nu(K)\setminus bound$.

A.2 Basis functions used for the DGTD schemes

On the reference cube $[-1,1]^3$ with coordinates (ξ,η,ζ). Let us denote by $(\mathbf{e}_i)_{i=1,\dots,6}$ the canonical basis of $\mathbb{R}^6$. The associated basis functions are:

- For the $FVTD$ scheme $(\mathbf{e}_i)_{i=1,\dots,6}$.
- For the first order Legendre P^1 scheme:
$$(\mathbf{e}_i)_{i=1,\dots,6}, (\xi\mathbf{e}_i)_{i=1,\dots,6}, (\eta\mathbf{e}_i)_{i=1,\dots,6}, (\zeta\mathbf{e}_i)_{i=1,\dots,6}.$$
- For the first order Lagrange Q^1 scheme:
$$((1-\xi)(1-\eta)(1-\zeta)/8\mathbf{e}_i)_{i=1,\dots,6}, ((1+\xi)(1-\eta)(1-\zeta)/8\mathbf{e}_i)_{i=1,\dots,6},$$
$$((1-\xi)(1+\eta)(1-\zeta)/8\mathbf{e}_i)_{i=1,\dots,6}, ((1-\xi)(1-\eta)(1+\zeta)/8\mathbf{e}_i)_{i=1,\dots,6},$$
$$((1-\xi)(1+\eta)(1+\zeta)/8\mathbf{e}_i)_{i=1,\dots,6}, ((1+\xi)(1-\eta)(1+\zeta)/8\mathbf{e}_i)_{i=1,\dots,6},$$
$$((1+\xi)(1+\eta)(1-\zeta)/8\mathbf{e}_i)_{i=1,\dots,6}, ((1+\xi)(1+\eta)(1+\zeta)/8\mathbf{e}_i)_{i=1,\dots,6}.$$
- For the P^1_{div} scheme ([3]):
$$\{(\mathbf{e}_i)_{i=1,\dots,6}, (\xi\mathbf{e}_i)_{i=2,3,5,6}, (\eta\mathbf{e}_i)_{i=1,3,4,6}, (\zeta\mathbf{e}_i)_{i=1,2,4,5}\}$$
- For the Q^1_{div} scheme ([13]):
$$((1-(\eta+1)/2)(1-(\zeta+1)/2)\mathbf{e}_i)_{i=1,4}, ((1-(\eta+1)/2)(\zeta+1)/2\mathbf{e}_i)_{i=1,4},$$
$$((\eta+1)/2(1-(\zeta+1)/2)\mathbf{e}_i)_{i=1,4}, ((\eta+1)/2(\zeta+1)/2\mathbf{e}_i)_{i=1,4},$$
$$((1-(\xi+1)/2)(1-(\zeta+1)/2)\mathbf{e}_i)_{i=2,5}, ((1-(\xi+1)/2)(\zeta+1)/2\mathbf{e}_i)_{i=2,5},$$
$$((\xi+1)/2(1-(\zeta+1)/2)\mathbf{e}_i)_{i=2,5}, ((\xi+1)/2(\zeta+1)/2\mathbf{e}_i)_{i=2,5},$$
$$((1-(\xi+1)/2)(1-(\eta+1)/2)\mathbf{e}_i)_{i=3,6}, ((1-(\xi+1)/2)(\eta+1)/2\mathbf{e}_i)_{i=3,6},$$
$$((\xi+1)/2(1-(\eta+1)/2)\mathbf{e}_i)_{i=3,6}, ((\xi+1)/2(\eta+1)/2\mathbf{e}_i)_{i=3,6}.$$